

## Chemical Reaction Dynamics of Dioxin Decomposition by Tight-Binding Quantum Chemical Molecular Dynamics Method

Ai Suzuki<sup>1</sup>, Tomonori Kusagaya<sup>1</sup>, Akira Endou<sup>1</sup>, Seiichi Takami<sup>1</sup>, Momoji Kubo<sup>1,2</sup>,  
Manogaran Sadasivam<sup>1</sup>, Akira Imamura<sup>3</sup> and Akira Miyamoto<sup>1,4,\*</sup>

<sup>1</sup>Department of Applied Chemistry, Graduate School of Engineering, Tohoku University, Aoba-yama 07, Aoba-ku, Sendai 980-8579, Japan

<sup>2</sup>PRESTO, Japan Science and Technology Agency, 4-1-8 Honcho Kawaguchi, Saitama 332-0012, Japan

<sup>3</sup>Department of Mathematics, Faculty of Engineering, Hiroshima Kokusai Gakuin Univ., 6-20-1 Nakano, Aki-ku, Hiroshima 739-0321, Japan

<sup>4</sup>New Industry Creation Hatchery Center, Tohoku University, Aoba-yama 10, Aoba-ku, Sendai 980-8579, Japan

\* Fax: +81-22-217-7235, e-mail: miyamoto@aki.che.tohoku.ac.jp

Elementary decomposition process of 2,3,7,8-tetra-chlorinated dibenzo-*p*-dioxin (2,3,7,8-TCDD) on V<sub>2</sub>O<sub>5</sub> catalyst was clarified for the first time at electronic level by using our tight-binding quantum chemical molecular dynamics (TB-QCMD) method with first-principles parameterization. This method realizes over 5000 times acceleration compared to the traditional first-principles molecular dynamics method. At 300 K the 2,3,7,8-TCDD adsorbed on the V<sub>2</sub>O<sub>5</sub>(010) catalyst, and especially its hydrogens were strongly attracted toward the terminal V=O bond of the catalyst. Hence, the structure of the 2,3,7,8-TCDD was bent, however its decomposition was not observed. When the temperature was increased to 473 K, first the C-C bond of the 2,3,7,8-TCDD was broken, and then the C-O bond dissociation was noticed. Moreover, the elongation of the terminal V=O bond of the catalyst was observed. The above bond-breaking and bond-elongation process were discussed in detail by using the change in the bond population during the QCMD simulation. Finally, these results indicate that the destruction process of the 2,3,7,8-TCDD starts from the C-C bond-breaking and then the C-O bond dissociation follows. The structure and electronic state changes of the catalysts by the adsorption and decomposition of the 2,3,7,8-TCDD were also analyzed.

Key words: dioxin, vanadium pentoxide, catalytic decomposition, tight-binding quantum chemical molecular dynamics, chemical reaction dynamics

### 1. INTRODUCTION

TiO<sub>2</sub>-based V<sub>2</sub>O<sub>5</sub> catalyst was originally utilized and industrialized for the removal of nitrogen oxides (NO<sub>x</sub>) by the selective catalytic reduction process. Moreover, recently it was shown that this catalyst is also effective for the decomposition of polychlorinated dibenzo-*p*-dioxin (PCDD) at the same temperature range with the deNO<sub>x</sub> reaction. However, the mechanism of the decomposition process of the PCDD on the above catalysts has not been well clarified. Hence, in order to design highly active catalysts for the PCDD decomposition, the electronic-level investigation of the decomposition process of the PCDD is strongly demanded.

First-principles molecular dynamics method [1] is one of the candidates to clarify the catalytic reaction dynamics at electronic level, however this method is computationally very costly. Therefore, Laasonen and Nieminen [2] proposed tight-binding quantum chemical molecular dynamics (TB-QCMD) approach based on the tight-binding approximation, which is much faster than the traditional first-principles molecular dynamics method.

Before their proposal, tight-binding approximation has been well improved by several approaches such as adding two-body repulsive energy term [3], distance-dependent Wolfsberg-Helmholz formula [4],

self-consistent-charge and self-consistent-configuration methods [5,6], *ab initio* parameterization [7-9] and so on. We integrated these improvements into the TB-QCMD method and then we succeeded in the development of novel TB-QCMD code "Colors". This program realizes over 5000 times acceleration compared to the traditional first-principles molecular dynamics method. Hence, it enables us to employ large catalyst model for the QCMD simulation, which cannot be done by the first-principles molecular dynamics method. Moreover, in order to realize high accuracy, all the parameters for the TB-QCMD simulations were determined on the basis of the first-principles calculation results.

Hence in the present study, we applied our original TB-QCMD method to the investigation of the elementary decomposition process of the 2,3,7,8-tetra-chlorinated dibenzo-*p*-dioxin (2,3,7,8-TCDD) on the V<sub>2</sub>O<sub>5</sub>(010) catalyst and its decomposition mechanism was discussed in detail. Moreover, the temperature effect was also investigated.

### 2. METHOD

#### 2.1. Tight-binding quantum chemical molecular dynamics

Our original TB-QCMD program "Colors" was employed for the present purpose. Total energy, *E*, is given by the following expression:

$$E = \sum_{i=1}^n \frac{1}{2} m_i v_i^2 + \sum_{k=1}^{occ} \varepsilon_k + \sum_{i=1}^n \sum_{j=i+1}^n Z_i Z_j e^2 / R_{ij} + \sum_{i=1}^n \sum_{j=i+1}^n E_{rep}(R_{ij}) \quad (1)$$

where the first, second, third, and fourth terms represent the kinetic energy of the nucleus, the summation of the eigenvalues of all occupied orbitals, the Coulombic interaction, and the short-range exchange-repulsion interaction, respectively. Here,  $m$  and  $v$  are mass and velocity of atoms,  $Z_i$  and  $Z_j$  are the charges of atoms,  $e$  is the elementary electric charge, and  $R_{ij}$  is the internuclear distance. The short-range exchange-repulsion term,  $E_{rep}(R_{ij})$ , is given by:

$$E_{rep}(R_{ij}) = b_{ij} \exp[(a_{ij} - R_{ij}) / b_{ij}] \quad (2)$$

where  $a_{ij}$  and  $b_{ij}$  are parameters related to the size and stiffness of the atoms, respectively. From the derivative of the Eq. (1), we obtain the following atomic force equation:

$$F_i = \sum_{j \neq i} \sum_{k=1}^{occ} C_k^T \left( \frac{\partial H}{\partial R_{ij}} \right) C_k + \sum_{j \neq i} \sum_{k=1}^{occ} \varepsilon_k C_k^T \left( \frac{\partial S}{\partial R_{ij}} \right) C_k - \sum_{j \neq i} Z_i Z_j e^2 / R_{ij}^2 + \sum_{j \neq i} \partial E_{rep}(R_{ij}) / \partial R_{ij} \quad (3)$$

where  $H$  is the Hamiltonian matrix,  $S$  is the overlap integral matrix,  $C$  is the eigenvector matrix, and  $C^T$  is the transformation matrix of the eigenvector matrix.

## 2.2. First-principles parameterization for TB-QCMD

In order to accelerate the calculation speed, we employed several parameters for the Hamiltonian in the TB approach. All the parameters were determined on the basis of the density functional theory (DFT) calculation results in order to realize high accuracy. Here, Amsterdam Density Functional (ADF) program [10] was employed for the first-principles parameterization. For the ADF calculations, triple zeta plus polarization functions (TZpp) basis sets were used and the energies were evaluated by the generalized gradient approximation with Becke-Perdew [11,12] functionals.

The Slater exponent  $\zeta_i$  of atomic orbital  $i$  is an important parameter for our TB approach. The Slater exponent values depending on the atomic charges were calculated by the DFT method and the charge-dependent results were fitted by polynomial functions.

The valence state ionization potential (VSIP) is employed as the parameter for the diagonal element of Hamiltonian,  $H_{rr}$ . On the basis of the improvement in the Wolfsberg-Helmholz formula by Anderson [13] and Calzafferi et al. [3], we used the following expression for  $H_{rs}$ :

$$H_{rs} = \frac{1}{2} K_{rs} (H_{rr} + H_{ss}) S_{rs} \quad (4)$$

$$K_{rs} = 1 + (\kappa_{rs} + \Delta^2 - \Delta^4 \kappa_{rs}) \exp[-\delta_{rs} (R_{ij} - d_0)] \quad (5)$$

$$\Delta = (H_{rr} - H_{ss}) / (H_{rr} + H_{ss}) \quad (6)$$

where  $d_0$  denotes the sum of the orbital radii.  $\kappa_{rs}$  and  $\delta_{rs}$  are parameters for the orbital-orbital interactions.

Similar to the derivation of the Fock matrix in the unrestricted Hartree-Fock equation, we derived the Eqs.

(7)-(10) for the spin-dependent Hamiltonian matrix for the TB-QCMD method.

$$H_{rr}^\alpha = H_{rr} - \frac{1}{2} (P_{rr}^\alpha - P_{rr}^\beta) (rr | rr) \quad (7)$$

$$H_{rr}^\beta = H_{rr} + \frac{1}{2} (P_{rr}^\alpha - P_{rr}^\beta) (rr | rr) \quad (8)$$

$$H_{rs}^\alpha = \frac{1}{2} K_{rs} (H_{rr} + H_{ss}) S_{rs} - \frac{1}{2} (P_{rs}^\alpha - P_{rs}^\beta) (rr | ss) \quad (9)$$

$$H_{rs}^\beta = \frac{1}{2} K_{rs} (H_{rr} + H_{ss}) S_{rs} + \frac{1}{2} (P_{rs}^\alpha - P_{rs}^\beta) (rr | ss) \quad (10)$$

Here, the parameter  $(rr|rr)$  was determined by the DFT method, while  $(rr|ss)$  was calculated using Nishimoto-Mataga's equation [14]. The  $H_{rr}$  and  $(rr|rr)$  values depending on the atomic charges were calculated by the DFT method. The charge-dependent results were fitted by polynomial functions and these values were used as the parameters for the TB-QCMD calculations. We also determined  $K_{rs}$ , namely  $\kappa_{rs}$  and  $\delta_{rs}$ , in Eqs. (4)-(6) for each atomic orbital pair on the basis of the DFT results.

In the conventional TB calculations, the total orbital energy is calculated by Eq. (11):

$$E = \sum_{k=1}^{occ} \varepsilon_k \quad (11)$$

where  $\varepsilon_k$  is the orbital energy. Taking into account the work by Anderson [15] and Anderson and Hoffman [16] for improving accuracy in the total valence electron energy, we introduced the following term as shown in Eq. (12). The  $\Delta E_i$  is added to the total energy calculation in Eq. (1). This parameter is determined for an individual atom with different charge. The DFT calculation results on the total energy of the single atom with different charges were utilized to determine the following parameters:

$$\Delta E_i = E_{DFT} - \sum_{k=1}^{occ} \varepsilon_k \quad (12)$$

However, the derivative of the  $\Delta E_i$  is very small and hence we neglect the contribution of  $\Delta E_i$  to the atomic force calculation.

## 2.3. TB-QCMD calculation conditions

The Verlet algorithm [17] was used for the calculation of atomic motions, while the Ewald method [18] was applied for the calculation of the electrostatic interactions under the three-dimensional periodic boundary condition. The NPT ensemble was realized by the scaling of the atom velocities and unit cell parameters. A constant pressure of 0.1 MPa and constant temperatures of 300 K and 473 K were employed, although the cell parameter of z-axis was fixed. A total of 3000 steps QCMD simulations were performed with time interval of 2 fs. The size of simulation cell and  $V_2O_5$  surface in this model are  $14.26 \text{ \AA} \times 11.52 \text{ \AA} \times 19.37 \text{ \AA}$  and  $14.26 \text{ \AA} \times 11.52 \text{ \AA} \times 4.75 \text{ \AA}$ , respectively. Dynamics of all the atoms in the  $V_2O_5$  catalyst and 2,3,7,8-TCDD were calculated without any constraints by our TB-QCMD method. The structures during the QCMD simulations were visualized using New-RYUGA program [19], which was developed in our laboratory.

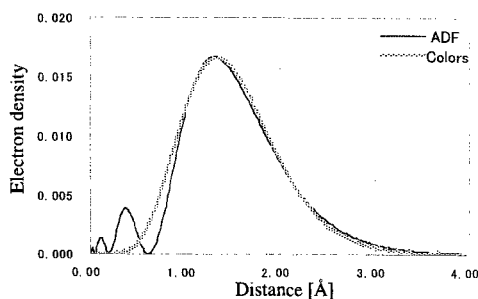


Figure 1. Comparison of the electron density of V 4s orbital obtained by ADF and Colors programs

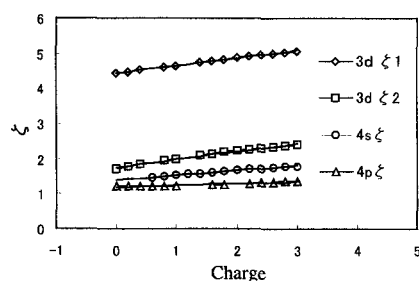


Figure 2. Slater exponents of V 3d, 4s and 4p orbitals depending on atomic charges

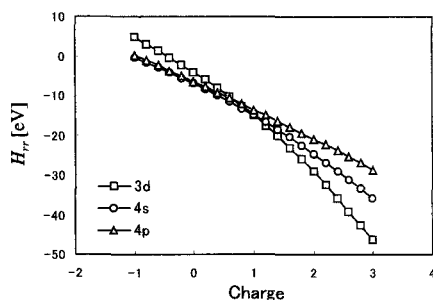


Figure 3.  $H_{rr}$  of V 3d, 4s and 4p orbitals depending on atomic charges

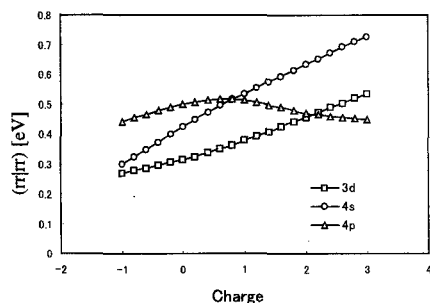


Figure 4.  $(rr|rr)$  parameters of V 3d, 4s, and 4p orbitals depending on atomic charges

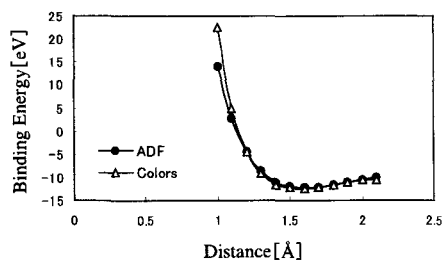


Figure 5. Comparison of the V-O diatomic potential curve obtained by ADF and Colors programs

### 3. RESULTS AND DISCUSSION

#### 3.1 First-principles parameterization by DFT

We employed the Slater-type orbital, which neglects the radial nodes in the TB-QCMD calculations. Our program uses a Slater-type orbital with single zeta for s and p orbitals and with double zeta for d orbitals. As an example, Fig. 1 shows that the V 4s single zeta Slater-type orbital obtained by colors program agreed well with the triple zeta orbital employed in the ADF calculations. The Slater exponents of V 3d, 4s, and 4p orbitals depending on the atomic charges were determined, as shown in Fig. 2. Here, double zeta orbital was employed only in the 3d orbitals. The results were fitted by polynomial functions and used as TB-QCMD parameters. The Slater exponents for other atoms were also determined in the same manner.

The VSIP depending on the atomic charges and spins was also calculated by the ADF program. Here, we separated the  $H_{rr}^{\alpha}$  and  $H_{rr}^{\beta}$  into two parts; namely the spin-independent term,  $H_{rr}$ , and the spin-dependent term,  $(rr|rr)$ , as shown in Eqs. (7) and (8). As an example, the results of  $H_{rr}$  and  $(rr|rr)$  are shown for V 3d, 4s, and 4p orbitals in Figs. 3 and 4, respectively.  $H_{rr}$  and  $(rr|rr)$  depending on the atomic charge were also fitted by polynomial functions.

Moreover, we determined  $K_{rs}$ , namely  $\kappa_s$  and  $\delta_{rs}$ , in Eqs. (4)-(6) for each atomic orbital pairs, so as to reproduce the diatomic potential energy curves obtained by the ADF calculations. As an example, Fig. 5 shows the potential curve of the V-O diatomic distance obtained by our TB-QCMD program, which is in good agreement with the ADF calculation results. Moreover, the similar results were also obtained for various diatomic molecules composed of H, C, Cl and V atoms.

#### 3.2. Dioxin adsorption on $V_2O_5$ catalyst surface at 300 K

TB-QCMD calculation for the 2,3,7,8-TCDD on the  $V_2O_5(010)$  catalyst was performed at 300 K. The simulation result is shown in Fig. 6. The 2,3,7,8-TCDD adsorbed on the  $V_2O_5(010)$  surface, and especially its hydrogens were strongly attracted toward the terminal V=O bond of the catalyst. Finally, the C atoms adjacent to the O atoms in the 2,3,7,8-TCDD attached to the  $V_2O_5$  catalyst surface. The structure of the 2,3,7,8-TCDD was significantly bent by its adsorption on the catalyst, however its decomposition was not observed at this low temperature of 300 K.

#### 3.3. Dioxin decomposition on $V_2O_5$ catalyst surface at 473 K

We increased the simulation temperature to 473 K in order to clarify the decomposition mechanism of the 2,3,7,8-TCDD on the  $V_2O_5(010)$  catalyst (Fig. 7). Here, we have to mention that this temperature is lower than the regular experimental condition. From this figure, we noticed that the decomposition process of the 2,3,7,8-TCDD on the  $V_2O_5$  catalyst was successfully simulated by our TB-QCMD method. In the present calculation, any constraints were not applied to the reaction path, which indicates that the above chemical reaction occurred spontaneously. This result shows that the decomposition of the 2,3,7,8-TCDD started from the

C-C bond-breaking of the benzene ring, which can be seen at 1450 step of Fig.7. Later, the C-O bond dissociation was observed at 2000 step of Fig. 7.

The analysis of the change in the bond population during the QCMD simulation is very effective to clarify the bond-breaking and bond-formation dynamics of the catalytic reactions. Hence, in order to analyze the detailed mechanism of the decomposition process of the 2,3,7,8-TCDD, the change in the bond population of the  $C_a-C_b$ ,  $C_c-O$ ,  $C-Cl$ , and other C-C bonds in the 2,3,7,8-TCDD as well as that of the terminal  $V=O$  bond were analyzed. Here, the position of  $C_a$ ,  $C_b$ , and  $C_c$  is shown in Fig. 7. It can be seen from Fig. 8 that  $C_a-C_b$  bond population were decreased after 1300 step and reached to almost zero at 1600 step. This result validates that the decomposition of the 2,3,7,8-TCDD started from the C-C bond-breaking of the benzene ring. After the decrement of the C-C bond population, the  $C_c-O$  bond population was also decreasing from 1500 step and

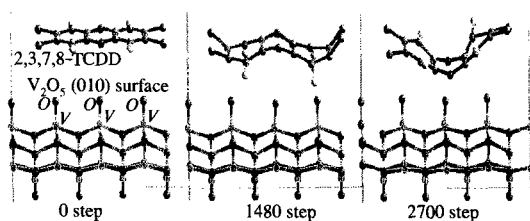


Figure 6. Dioxin adsorption on  $V_2O_5$  (010) surface at 300 K

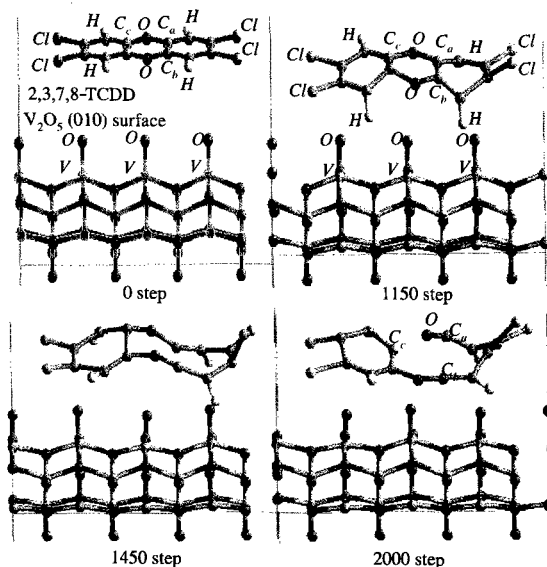


Figure 7. Dioxin decomposition on  $V_2O_5$  (010) surface at 473 K

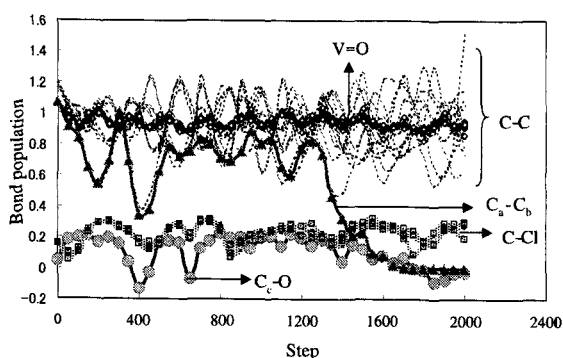


Figure 8. Change in the bond population of 2,3,7,8-TCDD and terminal  $V=O$  bond at 473 K

reached to zero at 1800 step. This result also confirms that the C-O bond dissociation followed after the C-C bond-breaking in the 2,3,7,8-TCDD. Whereas, the C-Cl bond population was stable, therefore it means that the chlorines of the 2,3,7,8-TCDD are difficult to be abstracted at this temperature of 473 K. Experimentally the abstraction of chlorines is observed, however we mention here that the above simulation temperature is quite lower than the regular experimental condition.

On the other hand, the elongation of the terminal  $V=O$  bond of the  $V_2O_5(010)$  catalyst was also observed and its population was slightly decreased. This result indicates that the structure and electronic states of the catalyst surface are also strongly influenced by the decomposition process of the 2,3,7,8-TCDD and it can be also well analyzed by our TB-QCMD approach.

#### 4. CONCLUSION

Our TB-QCMD method with first-principles parameterization successfully simulated the adsorption and decomposition process of the 2,3,7,8-TCDD on the  $V_2O_5$  catalyst. The temperature effect and detailed mechanism of its decomposition process were well clarified. Although further study is essential under the oxygen atmospheric condition, we confirmed that our new method is very effective to clarify the catalytic reaction dynamics at reaction temperatures.

#### References

- [1] R. Car and M. Parrinello, *Phys. Rev. Lett.*, **55**, 2471 (1985).
- [2] K. Laasonen and R. M. Nieminen, *J. Phys.: Condense Matter.*, **2**, 1509 (1990).
- [3] G. Calzaferri, L. Forss and I. Kamber, *J. Phys. Chem.*, **93**, 5366 (1989).
- [4] A. B. Anderson, W.G. Robin and Y.H. Sung, *J. Chem. Phys.*, **91**, 4245 (1987).
- [5] M. Zerner and M. Gouterman, *Theo. Chem. Acta.*, **4**, 44 (1966).
- [6] C. J. Ballhausen and H. B. Gray, "Molecular orbital theory", Benjamin, New York (1965).
- [7] P. Blaudeck, T. Frauenheim, D. Porezag, G. Seifert, and E. Fromm, *J. Phys. C*, **4**, 6389 (1992).
- [8] M. Menon and K. R. Subbaswamy, *Phys. Rev. B*, **47**, 12754 (1993); **50**, 11577 (1994).
- [9] N. Bernstein and E. Kaxiras, *Phys. Rev. B*, **56**, 10488 (1997).
- [10] E. J. Bearends, D. E. Elis and P. Ros, *Chem. Phys.*, **2**, 41 (1973).
- [11] A. D. Becke, *J. Chem. Phys.*, **98**, 1372(1993); *Phys. Rev. A*, **38**, 3098 (1988).
- [12] J. P. Perdew, J. A. Chevary, S. H. Vosko, K. A. Jackson, M. R. Pederson, D. J. Singh and C. Fiolhais, *Phys. Rev. B*, **46**, 6671 (1992).
- [13] A. B. Anderson, *J. Chem. Phys.*, **62**, 1187 (1975).
- [14] N. Mataga and K. Nishimoto, *Z. Physik. Chem. (Frankfurt)*, **12**, 335 (1957).
- [15] A. B. Anderson, *J. Chem. Phys.*, **60**, 2477 (1974).
- [16] A. B. Anderson and R. Hoffman, *J. Chem. Phys.*, **60**, 4271 (1974).
- [17] L. Verlet, *Phys. Rev.*, **159**, 98 (1967).
- [18] P. P. Ewald, *Ann. Phys.*, **64**, 253 (1921).
- [19] R. Miura, H. Yamano, R. Yamauchi, M. Katagiri, M. Kubo, R. Vetrivel and A. Miyamoto, *Catal. Today*, **23**, 409 (1995).